THE EVAPORATION OF VOLATILE LIQUIDS

by

Peter Kawamura
Donald Mackay
Department of Chemical Engineering and Applied Chemistry
University of Toronto
Toronto, Ontario

This report has not undergone detailed technical review by the Environmental Protection Service and the content does not necessarily reflect the views and policies of Environment Canada. Mention of trade names or commercial products does not constitute endorsement for use.

This unedited version is undergoing a limited distribution to transfer the information to people working in related studies. This distribution is not intended to signify publication and, if the report is referenced, the author should cite it as an unpublished report of the Branch indicated below.

Any comments concerning its content should be directed to:

Environmental Emergencies Technology Division
Technical Services Branch
Environmental Protection Programs Directorate
Environmental Protection Service
Environment Canada
Ottawa, Ontario
K1A 1C8

EE-59

April, 1985

ABSTRACT

Two evaporation models have been developed which can be used to estimate the evaporation rate of volatile as well as non-volatile liquids resulting from ground spills. Both models are based on steady state heat balances of the chemical pool and include effects of variables such as solar insolation and evaporative cooling. The simpler of the two, called the direct evaporation method, estimates the evaporation rate directly from available physical-chemical data. The second model, called the surface temperature method, determines the surface temperature of the evaporating pool by an iterative procedure. This temperature is then used to predict the evaporation rate.

A series of experiments was conducted in which the evaporation rates of five liquids: toluene, cyclohexane, hexane, dichloromethane, and pentane, were measured from pans under known meterological conditions. The two models agreed well with the experimental evaporation rates for the chemicals under both summer and winter environments. It was concluded that either model could be used to obtain a reasonable estimate of the evaporation rate under actual spill conditions.

An exploratory study of the evaporation rate of a chemical from snow was conducted in order to determine the best experimental approach to obtaining data and modelling this more complex situation.

LIST OF FIGURES

Figure		Page
1.1	Evaporation Rate of Pentane as a Function of Temperature	3
2.1	Steady State Energy Budget For an Evaporating Pool	10
2.2	Effective Solar Insolation as a Function of Cloud Cover and Solar Altitude	11
2.3	Atmospheric Radiation Factor	12
4.1	Evaporation Apparatus	21
4.2	Evaporation Measuring Device and Anemometer	21
4.3	Evaporation Experiment in Winter	22
4.4	Pyranometer and Other Instruments	22
4.5	Overall Experimental Apparatus	23
4.6	Snow Evaporation System	23
5.1	Comparison of Model Predictions and the Experimental Evaporation Rate	26
5.2	Evaporation of Toluene From Snow as a Function of Depth and Time	33
5.3	Depth-Averaged Evaporation of Toluene From Snow	33
5.4	Comparison of the Overall Evaporation Rates From Snow (cumulative) and From a Pool	34

LIST OF TABLES

Table		Page
3.1	Summary of Input Data and Assumptions for the Direct Evaporation Method and the Surface Temperature Method	18
5.1	Summary of Experimental Results and Model Predictions	25
5.2	Comparison of Mackay and Matsugu Mass Transfer Coefficient (km), With Experimental (kex)	28
5.3	Mass Transfer Coefficient and the Evaporation Rate	29

TABLE OF CONTENTS

		Page
ABSTRACT		i
RESUME		ii
LIST OF FIGURES		iii
LIST OF TABLES		iv
CONCLUSIONS		vii
1	INTRODUCTION	1
1.1	Importance of Evaporation Rate in Spill Situations	1
1.2	Evaporation Rate and the Wet Bulb Effect	1
1.3	Existing Evaporation and Spill Models	4
1.4	Objectives of This Study	5
2	THEORETICAL SECTION	6
2.1	Solar Radiation	6
2.2	Long-Wave Energy Exchange	7
2.3	Evaporation Energy	8
2.4	Sensible Heat Exchange	9
2.5	Other Sources of Energy	9
3	EVAPORATION MODELS	13
3.1	Direct Evaporation Method	13
3.2	Surface Temperature Method	16
4	EXPERIMENTAL	19
4.1	Evaporation Experiments	19
4.2	Evaporation Studies From Snow	20
5	RESULTS AND DISCUSSION	24
5.1	Evaporation Experimental Results and Model Predictions	24
5.2	Validity of Raphael's Solar Insolation Relationship	27
5.3	Mass Transfer Coefficients	27
5.4	Validity and Discussion of the Use of Evaporation Models Under Spill Conditions	30

		Page
5.5	Determining Which Model to Use	31
5.6	Exploratory Study of Evaporation From Snow	32
NOMENCLATURE		36
REFERENCES		37
ACKNOWLEDGEMENTS		39
APPENDIX A:	TIME ZONE FACTORS	40
APPENDIX B:	WIND VELOCITY CALCULATION	41
APPENDIX C:	EXPERIMENTAL DATA	42
APPENDIX D:	COMPUTER PROGRAM - DIRECT EVAPORATION MODEL	53
APPENDIX E:	COMPUTER PROGRAM - SURFACE TEMPERATURE MODEL	54

CONCLUSIONS

Two models, the direct evaporation equation and the surface temperature method were developed, which predict the evaporation rate of pure liquid chemicals resulting from ground spills. These models are relatively simple and based on available physical-chemical data. Their main advantage is that the effects of important variables, such as solar insolation and evaporative cooling are included.

Both models showed good agreement with experimental evaporation rates for five selected volatile chemicals under varying environmental conditions. The difference between the model predictions and the experimental rates ranged from 1 to 39% for the direct evaporation method and 1 to 30% for the surface temperature model. Since these models were found to have similar accuracy and applicability, either model could be used to predict the evaporation rate under spill conditions. It is recommended that studies on the magnitude and the duration of the effects of ground conduction be undertaken.

A simple experiment was performed to study the evaporation rate of toluene from snow. The overall rate of evaporation from snow was compared to the evaporation rate from a liquid pool of similar chemical volume as that in snow, as predicted by the direct evaporation model. The rate from snow decreased exponentially from an initial rapid rate of 220% to 25% of the rate from a pool after a 48 hour period. It is hoped that these preliminary results will be useful in conducting further research in this area.

1. INTRODUCTION

1.1 IMPORTANCE OF EVAPORATION RATE IN SPILL SITUATIONS

Accidental spills of hazardous and toxic chemicals during storage and transportation present a serious risk to the public's safety and to the environment. In particular, generation of excessive chemical vapour concentrations downwind of the accident may cause health problems and constitute a fire hazard, if the chemical is flammable. To establish the likely exposure concentration to the public and the possible effects on the environment, the evaporation rate of the chemical must be determined. This study is concerned with the prediction of the evaporation rate of pure volatile liquid chemicals resulting from ground spills, with particular emphasis on volatile liquids.

The evaporation rate determines the approximate time required for complete evaporation, given the initial spill volume. The knowledge of this period and the evaporation rate, along with the physical properties of the chemical, is necessary to implement proper mitigative procedures in an event of a spill, such as the need (if any) for an immediate clean-up of the spill, and the proper evacuation distances.

For example, if a relatively small amount of toluene was spilled on a hot summer day, it will evaporate at a fast rate. In this situation, it is best to allow the chemical to evaporate to completion, and evacuation may be necessary, depending on the actual evaporation rate, the prevailing atmospheric conditions, and the toxicity of the chemical, which are required for the atmospheric dispersion model in assessing "safe" distances from the spill area. On the other hand, if the same spill occured on a typical winter day in Canada, the evaporation rate may be slow such that the time required for complete evaporation is excessively long. Under these circumstances, it may be best to proceed with the appropriate clean-up procedures. Therefore, the estimation of the evaporation rate, evaluated under specific atmospheric and spill conditions is essential in dealing with spills of hazardous or toxic substances.

1.2 EVAPORATION RATE AND THE WET BULB EFFECT

The evaporation rate is dependent primarily on the vapour pressure of the chemical, evaluated at the surface of the chemical pool, and the evaporation mass transfer coefficient. The evaporation rate may be calculated by the following equation:

$$E = k M P(Ts) /(R Ts) \qquad (1.1)$$

in which E is the evaporation rate (g/m2 h), M is the molecular weight of the chemical (g/mol), P(Ts) is the vapour pressure of the chemical (Pa), R is the gas constant (8.314 Pa m3 /mol K), Ts is the surface temperature of the chemical pool (K), and k is the mass transfer coefficient (m/h). Mackay and Matsugu (1973) have determined this coefficient as a function of the wind speed, the diameter of the pool and the chemical's Schmidt number:

$$k = 0.029\ (u)^{0.78}\ (X)^{-0.11}\ (Sc)^{-0.67} \qquad (1.2)$$

in which u is the 10 m wind speed (m/h), X is the pool diameter (m), and Sc is the Schmidt number.

Thus, it is possible to calculate the evaporation rate using the above two equations. However, evaluating the vapour pressure of the chemical, which is the evaporation driving force, requires a knowledge of the surface temperature of the evaporating pool.

This surface temperature maybe difficult to estimate since it is a function of many variables, including solar insolation, evaporative cooling, and sensible heat transfer between the pool surface and the air, and between the pool and the ground. In general, the pool surface is lower than the average pool temperature, and the average pool temperature may be higher or lower than the air temperature. These differences may be small for relatively non volatile chemicals but can become significant when dealing with chemicals of high volatility.

Highly volatile chemicals, such as pentane and low molecular weight ethers, due to their high evaporation rate, have a large evaporative cooling effect. This results in lower surface and pool temperatures, relative to air temperature. This phenomenon is called the "wet bulb effect". On the other hand, moderately volatile chemicals, such as toluene, may have surface temperatures greater or less than the air temperature. The magnitude of the temperature depression or increase depends on the energy exchange between the pool and the environment. Thus, prevailing environmental conditions, as well as the physical-chemical properties of the chemical must be combined quantitatively to evaluate the surface temperature.

To illustrate the importance of the surface temperature in predicting the evaporation rate, an experiment was performed under environmental conditions in which pentane was allowed to evaporate from a flat pan. Figure 1.1 illustrates the evaporation rate calculated by using equation 1.1 by utilizing both the air temperature and the actual experimental surface temperature to evaluate the vapour pressure. It is clear from the figure that using the air temperature to determine the

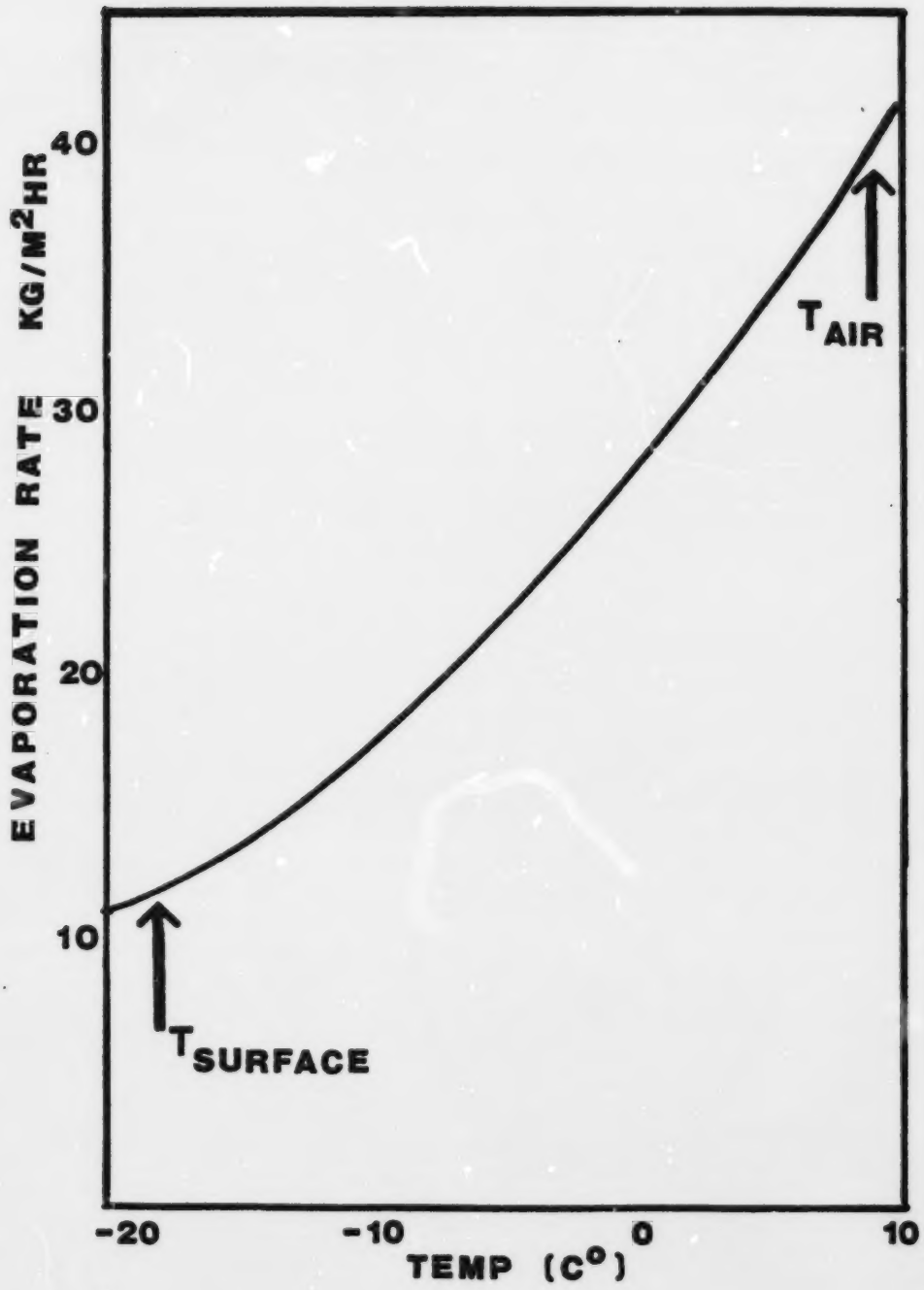

Figure 1.1: Evaporation Rate of Pentane as a Function of Temperature

vapour pressure will not result in a reasonable prediction of the evaporation rate. In this case, the predicted rate using the air temperature was approximately four times as great as the "actual" evaporation rate. This is due to the large wet bulb effect of pentane. Similar results can be expected for other volatile chemicals. Therefore, the wet bulb effect must be considered when predicting the evaporation rate of volatile chemicals.

1.3 Existing Evaporation and Spill Models

Models of evaporation rate of chemicals from ground spills have been developed by several workers. Of these, three models, the US Army (1982), ESL (1983), and AWS (1978), predict the steady state evaporation rate by a simple formula based on mass transfer theory, while others are more complicated and require a computer for use.

The US Army (1982) model determines the evaporation rate as a function of the Reynold's number, the Schmidt number, the wind speed, and the vapour pressure of the liquid spilled. Although the model can also calculate the area of the spill if it is not known, as a function of two types of surfaces (concrete and gravel), the effects of evaporative cooling and radiation are neglected.

The ESL (1983) model is very simple and can be used to estimate rapidly the evaporation rates for a variety of chemicals. This model introduces a volatility factor, which is defined as the ratio of the vapour pressure of the chemical of interest to that of a reference chemical, hydrazine. The product of this factor and an empirically derived second order pool temperature function replaces the vapour pressure term in the equation similar to equation 1.1. The major problem with this model is determining the pool or the surface temperature. Since no solution is given to this problem, the air temperature must be used. Another inherent problem with this model is the dependence of the volatility factor on temperature.

The AWS (1978) model is an empirical equation based on laboratory studies of hydrazine. The evaporation rate is calculated as a function of the wind speed and a constant, which is equal to the vapour pressure at a particular temperature. This model is inadequate for general use since it lacks the dependence on temperature.

Other models, such as those of Shell (1980) and Ille and Springer (1978, 1983) involve a relatively complicated computer program. The Shell model is an unsteady state computer model which estimates the concentration of the chemical vapour as a function of time and distance down-wind of instantaneously formed pools of liquids and liquefied gases, continuous spills,

and stacks. However, despite its lengthly computer program and procedure, the model neglects solar radiation and evaporative cooling, which are key variables for evaporation of volatile chemicals. The Ille and Springer model estimates the steady state evaporation rate of the hydrazine family propellants, which includes the effects of solar radiation, ground roughness and terrain, and evaporative cooling.

The major drawback of these two models is that the input parameters required, such as the collision integral, are not generally available, which severely limits their applicability. Another disadvantage is that these models are too complicated for use at the spill site. The programs are too lengthy to program on a hand-held calculator, and require at least a desk-top computer.

Recently, Stiver and Mackay (1984) identified two key variables, the Henry's constant and a term called the evaporative exposure, which enable the evaporation rate and the spill duration to be calculated. This approach, however, is not recommended for spills involving volatile chemicals since the model neglects radiation and the wet bulb effect.

If a chemical is spilled on a porous surface, such as sand, soil or snow, an additional problem arises. As long as the spilled liquid exists as a pool, the evaportion rate can be estimated by one of the existing evaporation models. It is also useful to be able to predict the behaviour of the chemicals as they are sorbed into the porous medium. Phyper and Mackay (1985) developed a simple model which estimates the behaviour of a chemical spilled on soil. It includes the processes of infiltration, interaction with ground water, sorption, evaporation, dissolution and degrading reactions. There are, however, no literature or models relating to the evaporation and the behaviour of chemicals spilled on snow.

1.4 Objectives of This Study

It is desirable to develop a simple formula or procedure which can reasonably predict the evaporation rate of pure liquid chemicals resulting from ground spills under various environmental conditions. Critical parameters, such as solar insolation and evaporative cooling must be included in the formulation procedure. The purpose of this study was the development of such a formula or procedure and its verification with actual experimental data. An exploratory study was also performed on the evaporation rate of a chemical spilled on snow.

2. THEORETICAL SECTION

An energy balance for a chemical pool under environmental conditions may be written in the following form:

$$Qsol + Qatm - Qsur - Qev - Qsen + Qext = Qt \qquad (2.1)$$

in which Qt is the increase in energy stored in the pool, Qsol is the net solar radiation (corrected for the amount reflected from the surface), Qatm is the long-wave radiation from the atmosphere absorbed by the pool, Qsur is the long-wave radiation emitted by the pool, Qev is the energy lost by evaporation, Qsen is the sensible heat exchange between the pool and the atmosphere, and Qext is any other source of energy into the pool. The units are kJ/m2 hr for all terms. These terms are illustrated in Figure 2.1 and are discussed in the following sections.

2.1 Solar Radiation

Estimating the effective solar radiation on a horizontal surface of the pool involves determining the difference between the total incident and reflected solar radiation as a function of cloud cover and solar altitude.

Solar altitude, or angular elevation above the horizon, is a function of the latitude, declination of the sun, and the hour angle of the sun. These terms are related by the following expression which enables solar altitude to be calculated for any hour of any day of the year:

$$\sin (SA) = \sin LA \sin D + \cos LA \cos D \cos h \qquad (2.2)$$

where SA is the solar altitude, in degrees; LA is the latitude, in degrees; D is the declination, in degrees; and h is the hour angle of the sun, in degrees. The declination of the sun may be determined for any given day from a current solar ephemeris. However, reasonable accuracy is obtained from one table that lists the declination for any year since declination of the sun varies only by a few minutes from year to year on corresponding dates (Raphael, 1962). The following formula may also be used (Lunde, 1980):

$$D = 23.45 \sin [\ 360\ (N-80)/\ 370\ ] \qquad (2.3)$$

where N is the day number of the year.

The hour angle of the sun, which is the hour from solar noon converted into degrees, is calculated by the following expression:

$$h = 15\ [\ 12 - (\ tl + tz - L/15 + EQ/60\ )] \qquad (2.4)$$

in which tl is the local standard time, in hours; tz is the time zone factor (see Appendix A); L is the longitude, positive for locations east of the prime meridian and negative for west, in degrees; and EQ is the equation of time, in minutes. The equation of time, similar to declination, varies from day to day during the year but one table may be used for any year for engineering calculations. Therefore, the solar altitude can be determined for any location at any time of the year.

Raphael has gathered standard radiation curves from various sources and plotted the net solar insolation on a horizontal surface as a function of cloud cover and solar altitude, which is presented in Figure 2.2. This relationship can be approximated by the following equation:

$$Qsol = 4000\ [1-0.0071\ (C)^2\ ](\sin SA - 0.1) \qquad (2.5)$$

where C is the cloud cover factor (C=0 for sky with no clouds, and C=10 for complete cloud cover). This equation is valid only for sin SA > 0.1. For sin SA < 0.1, the solar insolation is very small, and can be assumed to be negligible.

The net insolation is the difference between the total solar radiation (including diffuse and reflected sky radiation) and the reflected short-wave radiation from the surface of the pool. The reflective property was based on information obtained from the water surface.

Since reflectivities of most chemicals are unknown, the reflectivity of water may be used to approximate the reflectivity of most chemicals. Hooper (1984) states that the human eye is a good detector of the reflectivity of a material. Since most liquid chemicals are clear and have similar visual appearance as that of water, this approximation will be used for this study. Figure 2.2 or equation 2.5 can thus be used to estimate the net solar insolation incident on the surface of the spill.

2.1 Long-Wave Energy Exchange

Long-wave energy exchange involves the long-wave radiation from the atmosphere, Qatm, that is absorbed by the pool and Qsur, the long-wave radiation emitted at the surface of the pool. Both terms are calculated based on the Stefan-Boltzmann radiation law. The difference, Qsur - Qatm, is occasionally referred to as the effective back radiation, Qback.

The energy emitted from the surface is:

$$Qsur = e\ \sigma\ (Ts)^4 \qquad (2.6)$$

where e is the emissivity of the chemical,
σ is the Stefan-Boltzmann constant (2.04x10(-7)kJ/m2K4 h)
and Ts is the absolute surface temperature of the pool (K).

The emissivity term is required since the surface does not behave as a perfect black body. As before, the emissivity of the water surface, which has a value of 0.970 (Raphael, 1962), is used for the emissivity of the chemical since no emissivity data are available for most chemicals. This is supported by the fact that most natural surfaces have an emissivity close to unity (Brutsaert, 1982).

The energy from the atmosphere by long-wave radiation is:

$$Qatm = (1- r)\ B\ \sigma\ (Ta)^4 \qquad (2.7)$$

where r is the reflectivity of the surface with regard to long-wave atmospheric radiation, Ta is the absolute air temperature (K), and B is the atmospheric radiation factor.

Although the atmospheric radiation is a function of many variables, Anderson (1954) proposed an empirical relationship which correlates atmospheric radiation with air temperature, water vapour pressure, and cloud cover and height, which are, with the exception of cloud height, readily available or obtainable. A 10% accuracy was placed on this correlation. Raphael summarized and simplified Anderson's relationsips and the results are shown in figure 2.3 which plots atmospheric radiation factor B as a function of cloud cover and vapour pressure of water in air without regard to cloud height. This enables the estimation of the radiation factor from conditions that are easily observed.

The product of B and $\sigma(Ta)^4$ must be corrected for the reflection of atmospheric radiation. For a water surface, the reflectivity was found to be 0.03 (Raphael, 1962). Again, this value is recommended for clear, visually water-like chemicals.

2.3 Evaporation Energy

The energy required for evaporation is simply the product of the heat of vaporization and the rate of evaporation, ie:

$$Qev = E\ Hvap\ /\ M \qquad (2.8)$$

where E is the evaporation rate (g/m2 hr) and Hvap is the heat of evaporation (kJ/mol). Combining equations 2.8 with 1.1, the evaporation energy is:

$$Qev = k\ P(Ts)\ Hvap\ /RTs \qquad (2.9)$$

This energy loss due to evaporation accounts for the phenomenon known as the evaporative cooling effect.

2.4 Sensible Heat Exchange

Sensible heat transfer occurs when there is a difference in temperature between the air and the surface of the pool. It may be written in the form:

$$Qsen = U\ (Ts-Ta) \qquad (2.10)$$

where U is the heat transfer coefficient (kJ/m2 hr C), which is a function of wind speed, temperature, and other properties. Ta is the absolute temperature of the air.

2.5 Other Sources of Energy

This term may be employed to include other sources or sinks of energy that was not covered in the previous sections. One example is the effect of heat conduction from the ground, which will introduce an unsteady state term in the heat balance. This is not treated explicitly in this study but methods are being sought to include it without the assembly and solution of differential equations.

Another is the unsteady state sensible heat release as the liquid cools from its pre-spill temperature to the evaporation temperature. It is likely that the degree of vertical mixing in the pool enhances the liquid's thermal conductivity to the extent that the entire pool contents are at a temperature close to that of the surface. In such cases, the magnitude of the latter sensible heat term can be readily estimated.

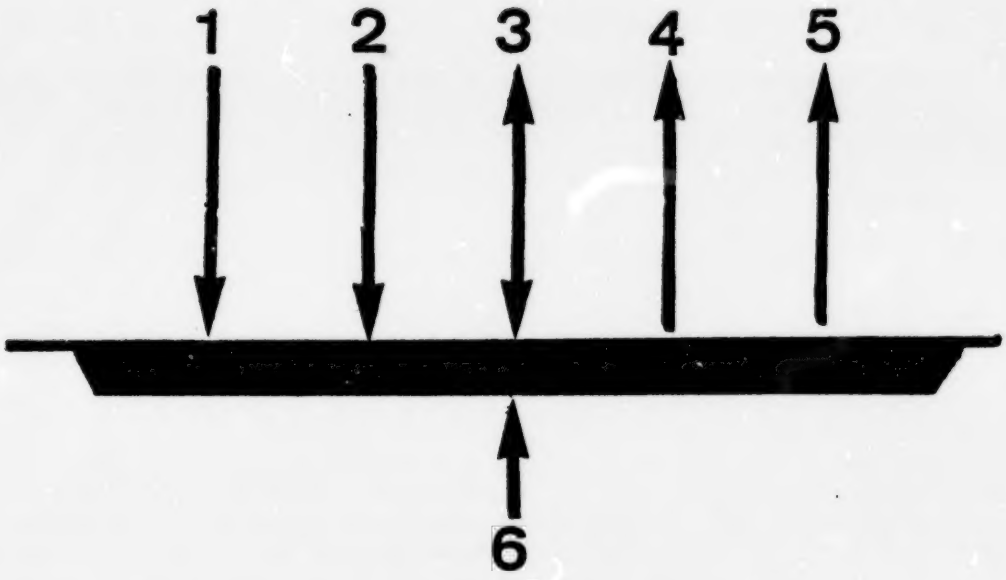

1 NET SOLAR RADIATION
2 ATMOSPHERIC RADIATION
3 SENSIBLE HEAT
4 EMITTED RADIATION
5 EVAPORATION ENERGY
6 GROUND CONDUCTION

Figure 2.1: Steady State Energy Budget For An Evaporating Pool

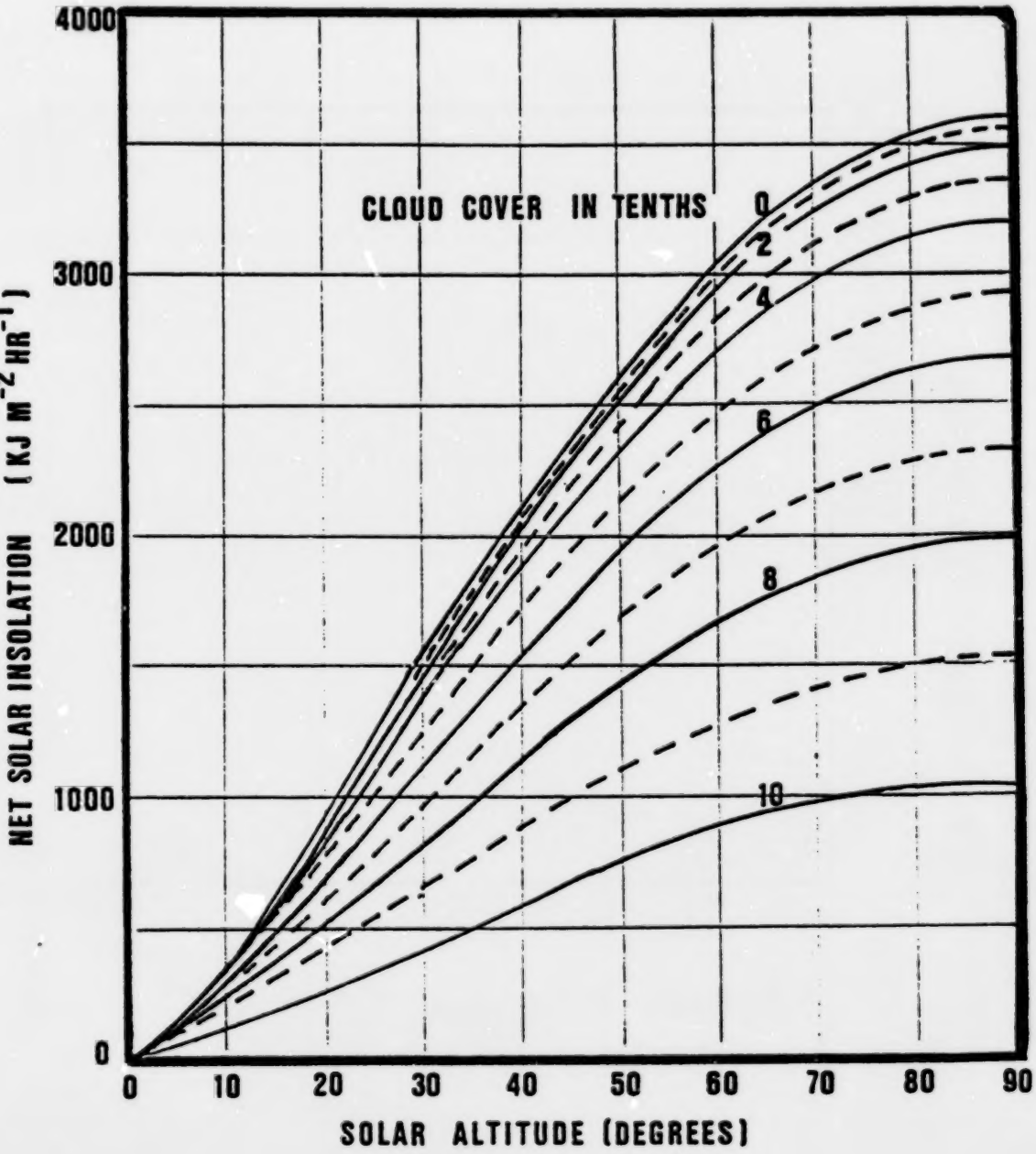

Figure 2.2: Effective Solar Insolation as a Function of Cloud Cover and Solar Altitude (Adapted from Raphael, 1962)

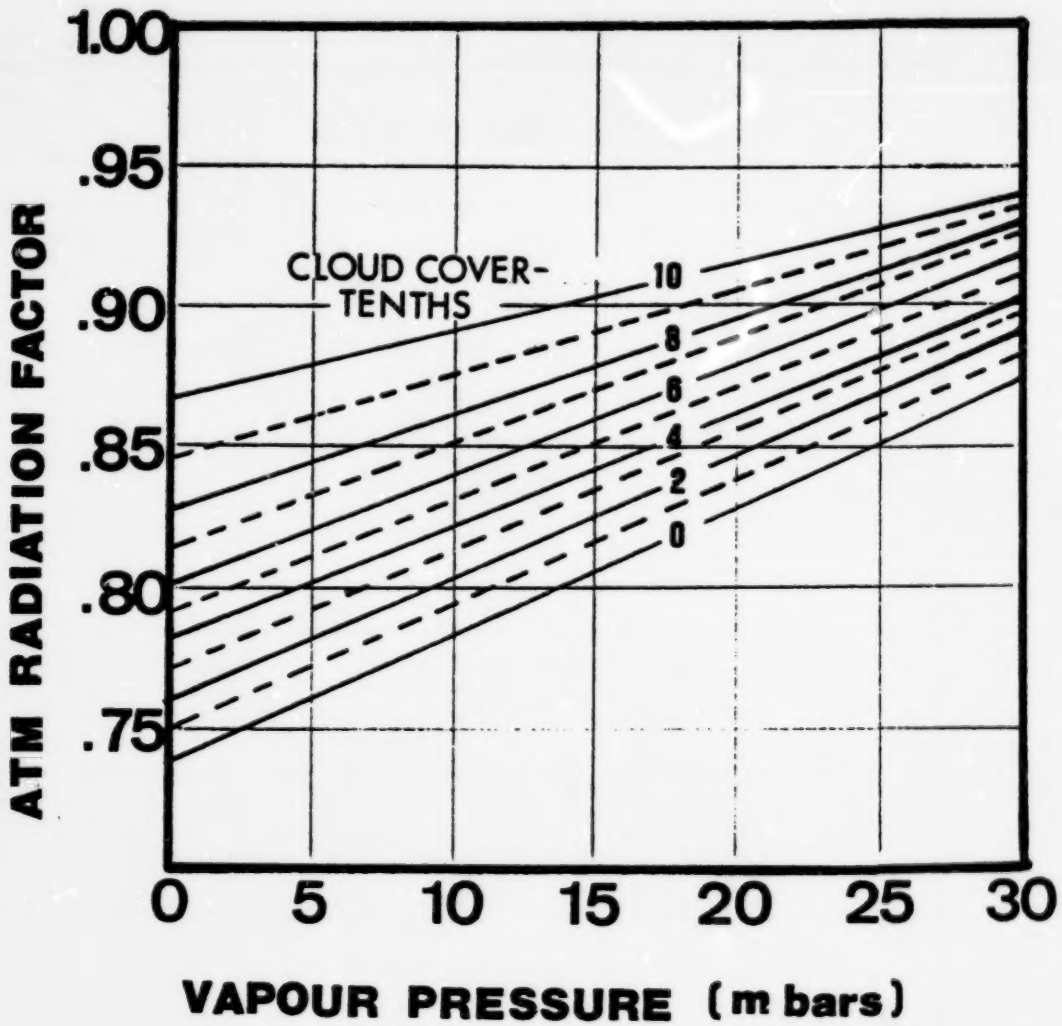

Figure 2.3: Atmospheric Radiation Factor
(Adapted from Raphael, 1962)

3. EVAPORATION MODELS

Two relatively simple evaporation models were assembled to predict the steady state evaporation rate from ground spills. These are the direct evaporation method and the surface temperature method. Both models include the effect of solar radiation as well as evaporative cooling, and the mass transfer coefficient of Mackay and Matsugu (equation 1.2) is employed.

The required parameters for the models, such as solar radiation and long wave energy exchange terms are determined from equations and diagrams presented in Section 2. Effects of sorption and conduction of heat from the ground are neglected in both models.

3.1 Direct Evaporation Method

This method is based on Penman's study of natural evaporation of water (1948). Few modifications have been made to adapt Penman's approach to the evaporation of a chemical under environmental conditions.

In studies relating to the evaporation of water, Bowen's ratio is frequently used. It is simply the ratio of the energy conducted to the pool as sensible heat from the air to the energy lost by evaporation. The Bowen's ratio, Bo, is:

$$Bo = Z\ (Ts-Ta)/(Ps-Pa) \qquad (3.1)$$

where Z is a constant,
P is the partial pressure of the substance with subscripts designating the surface (s), and the air (a).

This ratio is a useful tool in the development of a model to predict the evaporation rate of a chemical based on energy balance but it cannot be utilized in this form, since it contains terms dependent on the surface temperature, which is unknown. The objective was to introduce certain expressions for these terms based on simplifying assumptions, existing theory, and correlations, which will result in an explicit relationship between the evaporation rate and terms which can be easily determined. The development of this relationship is discussed in the following paragraphs.

The constant Z in the Bowen's ratio may be evaluated from equations 2.9 and 2.10 and from the heat and mass transfer analogy, which relates the heat and mass transfer coefficients by the following expression:

$$U = k\ \rho_a\ Cpa\ (Sc/Pr)^{0.67} \qquad (3.2)$$

where ρ_a is the density of air (mol/m3),
Cpa is the heat capacity of air (kJ/mol K),
Sc is the chemical Schmidt number
Pr is the Prandtl number.

The density of air is simply the atmospheric pressure divided by the gas constant and the absolute temperature. The ratio Z is:

$$Z = Patm\ Cpa\ (Sc/Pr)^{0.67} / Hvap \qquad (3.3)$$

where Patm is the atmospheric pressure (Pa), and the ratio has units of Pa/K. Since the Prandtl number and the heat capacity of air are relatively insensitive to temperature (Pr = 0.72 and Cpa = 0.029 kJ/mol K), the ratio is approximately:

$$Z = 3650\ (Sc)^{0.67} / Hvap \qquad (3.4)$$

To eliminate the surface temperature, Ts, which is unknown, the following assumption is made:

$$S = \left(\frac{dP^*}{dT}\right)_{Ta} \approx [P(Ts)-P(Ta)]/(Ts-Ta) \qquad (3.5)$$

where S is the slope of the vapour pressure curve for the chemical, and P* is the saturated vapour pressure. The slope is approximated by evaluating the derivative of the vapour pressure equation at the air temperature. It should be noted that the term Pa in the Bowen's ratio is negligible, since the concentration of the chemical in the bulk air phase is usually close to zero. This slope, for the vapour pressure equation of the form

$$\log_{10} P(t) = a + b/(t + c) \qquad (3.6)$$

with the temperature, t in Celsius is:

$$S = Y \exp [\ 2.3\ \{a+(b/(ta+c))\}\{-b/(ta+c)^2\}] \qquad (3.7)$$

where Y is the pressure conversion factor to Pa, and ta is the temperature of the air in Celsius.

It is useful to define a term, Q, which can be viewed as the amount of chemical that can be evaporated by the energy exchange with the environment:

$$Q = (Qsol + Qatm - Qsur + Qext)\ M / Hvap \qquad (3.8)$$

At this point, the ratios Z and S (identified by equations 3.4 and 3.7) are utilized in the steady state energy equation to

yield the following expression for Q:

$$Q = [1+(Z/S)]E - [(Z/S)\ (P(Ta)/P(Ts))]E \qquad (3.9)$$

The term P(Ts) can be eliminated by introducing equation 1.1 to the second term of the above equation. This yields:

$$Q = [1+(Z/S)]E - (Z/S)\ E(Ta) \qquad (3.10)$$

where E(Ta) is the "evaporation rate", which is based on the air temperature to evaluate the vapour pressure. Note that P(Ts) equals Ps; that is, the partial pressure of the chemical at the surface of the pool is equal to the saturated vapour pressure. E(Ta) is thus,

$$E(Ta) = k\ M\ P(Ta)/(R\ Ta) \qquad (3.11)$$

Finally, equation 3.10 can be rearranged to give an explicit relationship for the predicted evaporation rate, E, in g/m2 h. This relationship is:

$$E = [\ S/(Z+S)\ ]\ Q + [\ Z/(Z+S)\ ]\ E(Ta) \qquad (3.12)$$

The advantages of using this equation to predict the evaporation rate are (i) it includes the effects of solar insolation and evaporation cooling; (ii) it eliminates the need to determine the pool or surface temperature; (iii) it is simple (no iteration or computer requirement); and (iv) it is based on readily available physical-chemical data.

One drawback of this equation is that the long-wave radiation emitted by the surface of the pool, which is required for Q in equation 3.8 cannot be determined since this requires the knowledge of the surface temperature. However, this term is assumed to be approximately equal to the atmospheric radiation term under most conditions. Regardless of the magnitudes of these terms, the back radiation, Qback = Qsur-Qatm, is thought to be small compared to the other energy terms in the heat balance.

Based on this assumption, equation 3.10 is reduced to:

$$Q = (Qsol + Qext)\ M\ /\ Hvap \qquad (3.13)$$

A computer program of this model is included in Appendix D.

3.2 Surface Temperature Method

This method determines the surface temperature of the pool based on the steady state heat balance (equation 2.1 with Qt of zero). This temperature is then used to calculate the evaporation rate using equation 1.1.

The heat balance equation can be manipulated to yield the following:

$$0.97\,\sigma\,(Ts)^4 + Y\ k\ Hvap\ P(Ts)/(RTs) + U\ Ts =$$

$$Qsol + Qext + 0.97\ B\,\sigma\,(Ta)^4 + U\ Ta \qquad (3.14)$$

Note that the left hand side of the above equation consists of terms which depend on the unknown surface temperature, whereas on the right hand side, the terms can be easily evaluated. (The value for U may be determined by equation 3.2) If the right hand side of equation 3.14 is designated as a constant F, the equation becomes:

$$0.97\,\sigma\,(Ts)^4 + Y\ k\ Hvap\ P(Ts)\ /(RTs) + U\ Ts - F = 0 \qquad (3.15)$$

where

$$F = Qsol + Qext + 0.97\ B\ \sigma\,(Ta)^4 + U\ Ta \qquad (3.16)$$

Equation 3.15 may be solved for Ts by standard root determining methods such as Newton's, bisection, and globally convergent methods. This root, which is the predicted surface temperature of the pool, is used to calculate the evaporation rate using equation 1.1. This procedure is best suited for a computer but the program required is very short and simple.

Of the methods available to solve for the surface temperature, Newton's method may be best suited for this problem since it is very simple and often converges to the desired root rapidly. For example, for an "accuracy" of 0.5 C in the surface temperature, which is a reasonable estimate, considering other uncertainties involved, only a few iterations are necessary, depending on the choice of the initial guess of Ts. This first estimate may be taken to be the air temperature. A sample program utilizing the Newton's method is included in Appendix E.

Despite having to use a computer or a programmable calculator in this procedure, this method has the advantage of including all the energy exchange terms that are listed in the overall energy balance. If the assumptions made in the direct

evaporation formula development are found to be invalid under certain conditions, this method should be implemented under these conditions. The general approach taken was to obtain experimental data, test the two models and select the better on the bases of accuracy and convenience. A summary of input parameters required and the assumptions of the two models are listed in Table 3.1.

Table 3.1: A Summary of Input Data and Assumptions for the Direct Evaporation Method and the Surface Temperature Method

	Direct Evap.	Surface Temp.
INPUT DATA		
1. Physical Properties of the Chemical		
Vapour Pressure Equation	X	X
Heat of Vaporization (at air temperature)	X	X
Diffusivity in Air (to evaluate Schmidt No.)	X	X
Molecular Weight	X	X
Density	X	X
2. Atmospheric Properties		
Air Temperature	X	X
Density of Air	X	X
Viscosity of Air	X	X
10 m Wind Speed	X	X
Relative Humidity		X
Cloud Cover	X	X
Solar Altitude	X	X
3. Other Data		
Pool Area	X	X
Pool Diameter or Length	X	X
BASIC ASSUMPTIONS		
Steady State	X	X
No Ground Conduction	X	X
No Net Long-wave Energy Contribution-	X	
Pure Liquid Chemicals	X	X

4. EXPERIMENTAL

4.1 Evaporation Experiments

Evaporation experiments were performed at the Environment Canada Atmospheric Environment Services site in Woodbridge, Ontario, except during the period of August to September 1984, in which it was undertaken on the roof of the Chemical Engineering building of the University of Toronto. The procedure involved evaporating a chemical from an insulated circular pan under varying seasonal and atmospheric conditions. The following chemicals were used: toluene, cyclohexane, pentane, dichloromethane, and hexane. A photograph of the evaporation apparatus is shown in Figure 4.1.

The apparatus consited of a circular galvanized sheet-metal pan with the inner surface painted black. Two sizes of pans were used with the following diameters: 0.61 m (2 ft) and 0.91 m (3 ft). The depth of both pans was 5 cm. The choice of the size of the pan used in the experiment was based on the relative volatility of the chemical and the prevailing atmospheric conditions. The selected pan was placed on a styrofoam board to avoid heat conduction from the ground. The evaporation rate was measured by an evaporation measuring device which consists of a 6L glass reservoir, initially filled with the chemical, and a connecting glass tube, as shown in Figure 4.2. This device maintains a constant level of chemical in the evaporation pan by replacing the evaporated chemical by additions of chemical from the reservoir. Therefore, the evaporation rate was measured by observing the volume changes in the reservoir over a certain time period. A picture of this apparatus and the overall experimental equipment are shown in figures 4.2 to 4.5.

During the experiment, the evaporation rate and the bulk pool and surface temperatures were measured. The latter was accomplished by placing a thin copper-constantan thermocouple at the surface of the pool. The surface temperature was continuously recorded by a chart recorder. Furthermore, atmospheric data, such as solar insolation, and the average wind speed, were measured by an Epply pyranometer and an cup-counter anemometer, respectively. The wind speeds obtained from the anemometer were adjusted to a height of 10 m (refer to Appendix B for calculation). The air temperature and the cloud cover were also recorded. The relative humidity of the atmosphere was obtained from the weather office.

The data obtained from the experiment were averaged over a defined time interval. Experimental values of air temperature, extrapolated 10 m wind speed, cloud cover and relative humidity

were used as inputs to the two evaporation models. The difference between the bulk pool temperature and the reservoir temperature was utilized to compute the "external" source/sink of heat, which was used in the models. The model predictions were then compared to the experimental evaporation rate.

The other experimental data were used to calculate and compare the existing equations and correlations to the experimentally determined values. For example, the measured solar radiation was compared with Raphael's solar radiation curve (Figure 2.2), and the mass transfer coefficient of Mackay and Mastugu was tested against the actual mass transfer coefficient calculated from the measured surface temperature.

4.2 Evaporation Studies From Snow

A simple experimert was performed at the roof of the Chemical Engineering building of the University of Toronto to study the evaporation rate of a chemical from snow. The selected chemical was toluene.

Fresh snow was handpacked into a plastic circular cylinder, 40 cm in diameter and 20 cm in length. The density of the packed snow was 0.4 g/mL. A screen was placed on the bottom of this cylinder containing the snow. To this snow, which was firmly suspended above the ground, approximately 7L of toluene (initial temperature of 1 degree C), was added. The excess chemical was allowed to drain from the steel screen and the now-saturated snow was placed on top of a wooden board. A sample of the snow was taken at this point to determine the initial concentration of toluene. Additional snow was packed around the plastic cylinder to prevent heat transfer through the sides. This apparatus was left on top of the roof for a period of 48 hours, during which time 5 samples were taken. A photograph of the system is presented in Figure 4.6.

The snow-toluene samples were taken using an 8 cm diameter glass cylinder with a length of 20 cm. The sample was then immediately divided into four-5 cm layers, with each layer yielding a sample corresponding to a certain depth. Each portion was melted and the relative amount of toluene was determined. Average values for the atmospheric properties, such as the air temperature, and the wind speed were obtained throughout the experimental period from the weather office.

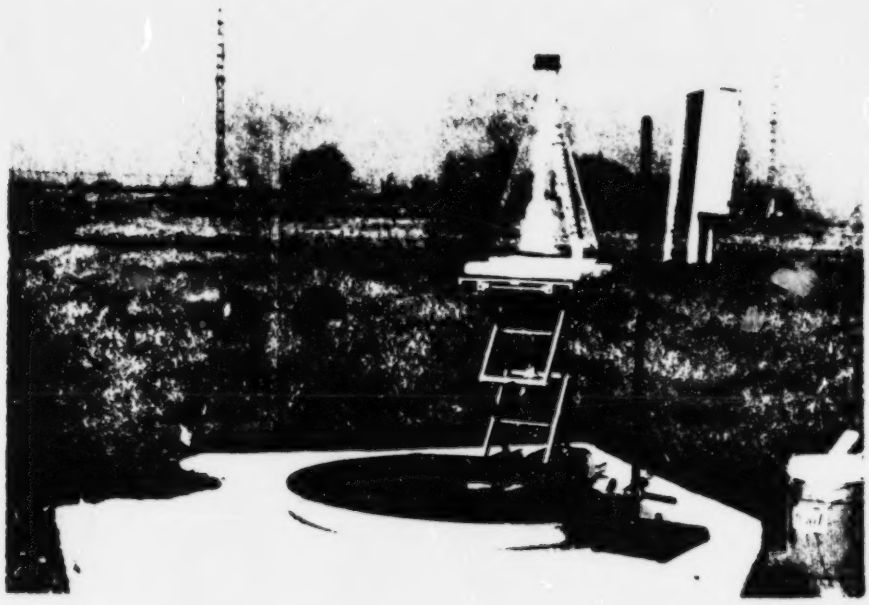

Figure 4.1: Evaporation Apparatus

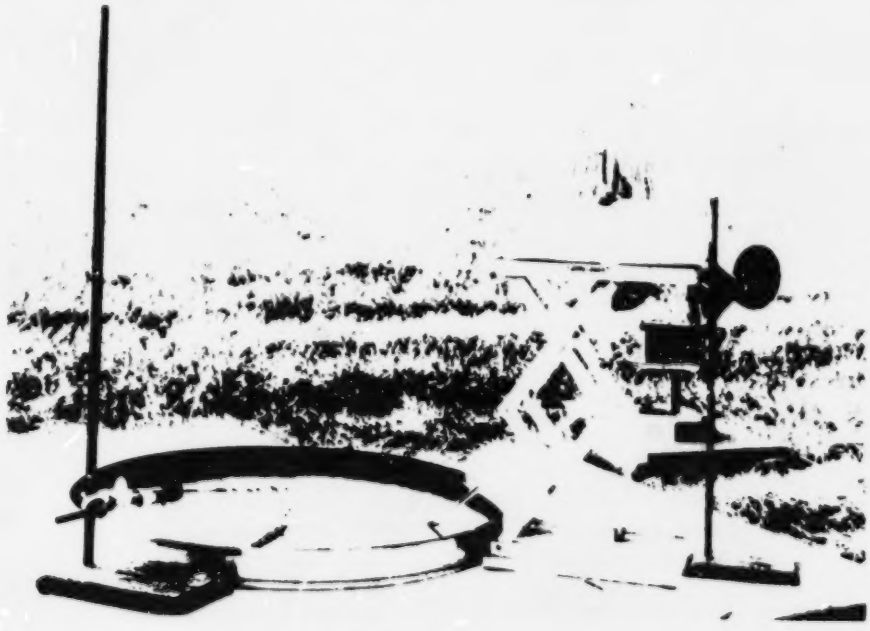

Figure 4.2: Evaporation Measuring Device and Anemometer (background)

Figure 4.3: Evaporation Experiment in Winter

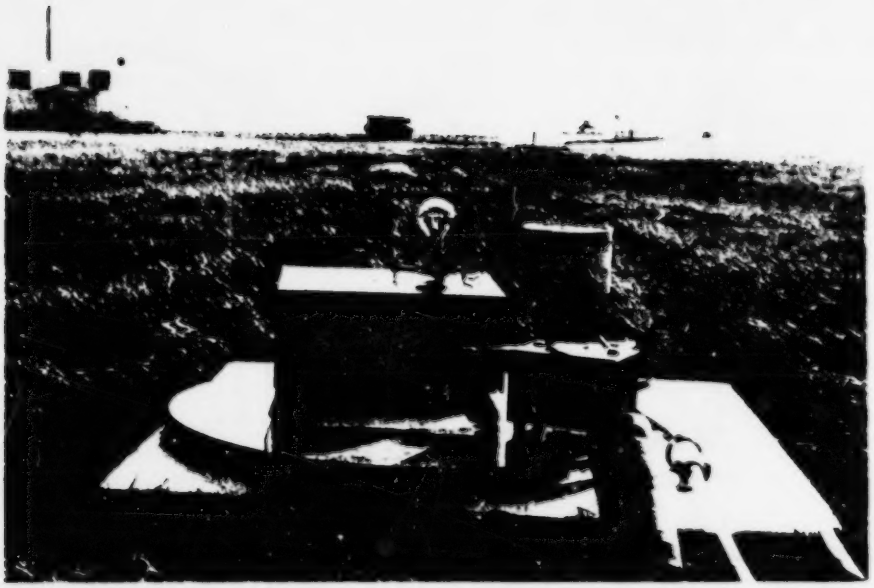

Figure 4.4: Pyranometer and Other Instruments

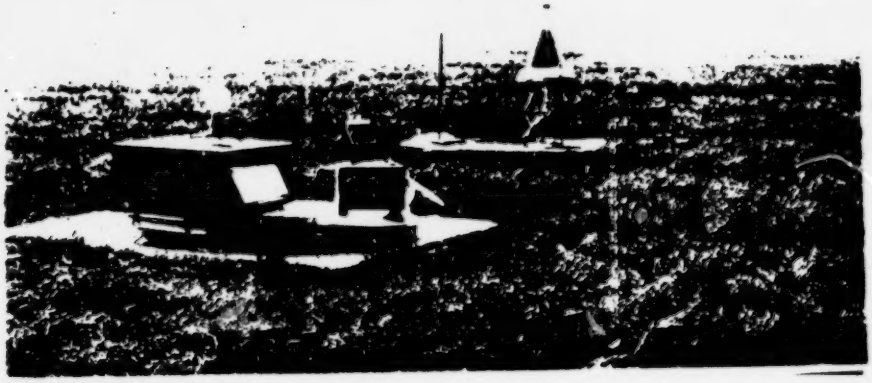

Figure 4.5: Overall Experimental Apparatus

Figure 4.6: Snow Evaporation System

5. RESULTS AND DISCUSSION

5.1 Evaporation Experimental Results and Model Predictions

The experimental data were averaged over a time period of one half to one hour for each experiment after "steady state" conditions were reached. The specific time interval depended on the duration of the experiment, which lasted from one to three hours. During this time, up to 6L of the chemical were evaporated.

Steady state condition was defined as the time after initial filling of the evaporation pan with the chemical when the pool temperature did not change by a rate greater than 2 degrees C over a 5 minute period. The initial temperature of the chemical was approximately equal to the ambient temperature for all experiments. For experiments involving very volatile chemicals, such as hexane, dichloromethane, and pentane, the pool temperature decreased rapidly after initial filling of the pan. In most experiments, "steady state" was reached in less than 15 minutes after commencement of the experiment. This is discussed further in Section 5.4.

The results from the evaporation experiments were compared to the evaporation rates predicted by the direct evaportion and the surface temperature models. This comparison is illustrated in Figure 5.1 and the actual evaporation rates as well as the air temperature under which the experiments were performed are given in Table 5.1 in the order of increasing volatility of the chemicals used. See Appendix C for further details of experimental data.

The results in Table 5.1 suggest that both the direct evaporation method and the surface temperature method predicted evaporation rates which generally agreed well with the experimental evaporation rates under both summer and winter conditions. The difference between the predicted and the experimental rates varied from 1 to 39% for the direct evaporation method and 1 to 30% for the surface temperature method, which is reasonable for models applied under environmental conditions.

The results also indicate that neither model is significantly more accurate than the other. The two model's predictions for moderately volatile chemicals (experiment no. 1 to 4) were excellent, except for experiment no. 2. In the experiments involving very volatile chemicals (no. 5 to 11), closer investigation reveals that only one of the two models was able to predict the evaporation rate with less than 15% difference for each of the seven experiments. The model in which the better results were obtained was the direct evaporation model for five and surface temperature model for two of these

Table 5.1: Summary of Experimental Results and Model Predictions

Exp No.	Chemical	Air Temp (C)	---- MODEL PREDICTIONS ---- Direct Evap.	%Dif	Surface Temp.	%Dif	Exper. Evap. Rate
1	Toluene	21	4.52	1	4.59	2	4.49
2	Toluene	29	4.70	39	4.39	30	3.39
3	Cyclohexane	24	6.47	10	5.59	5	5.89
4	Cyclohexane	25	6.61	12	5.97	1	5.89
5	Hexane	-5	7.00	26	6.10	10	5.55
6	Dichl.methane	-6	12.42	31	10.23	8	9.49
7	Dichl.methane	1	6.69	11	6.07	19	7.53
8	Pentane	1	9.36	11	8.14	23	10.52
9	Pentane	5	6.31	8	5.68	17	6.84
10	Pentane	7	7.07	13	6.44	21	8.13
11	Pentane	9	9.18	12	8.16	22	10.41

* The evaporation rates are in kg/m2 h.

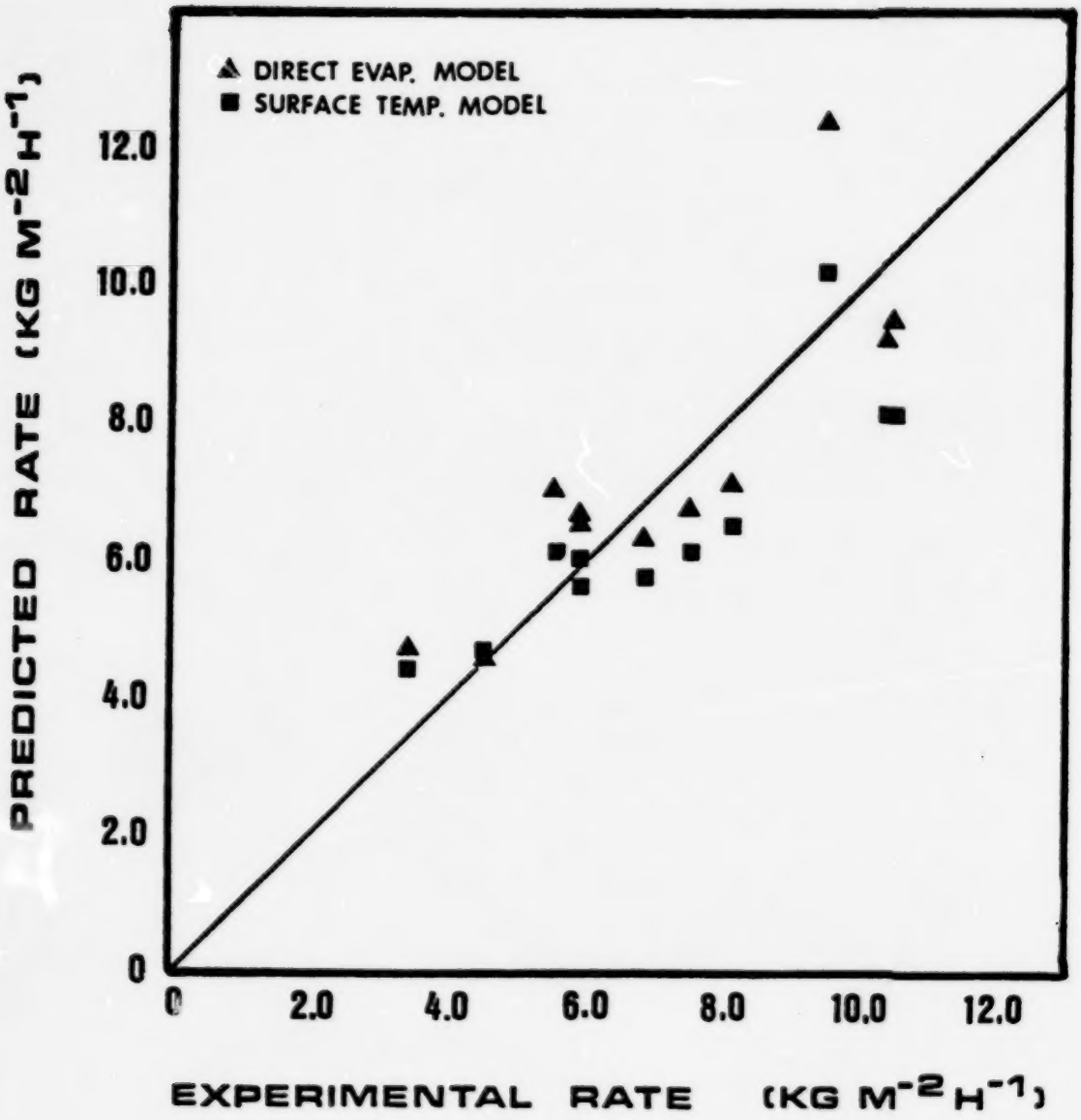

Figure 5.1: Comparison of Model Predictions and the Experimental Evaporation Rate

experiments. Despite the fact that the direct evaporation method was frequently "more accurate" for very volatile chemicals, the surface temperature method incurred a slightly lower overall prediction error. Thus, from Table 5.1, there is no basis to suggest that one of the models is superior in terms of accuracy.

Furthermore, there are no definite trends to the predicted evaporation rates, as seen in Figure 5.1. Both models underpredicted the evaporation rates for pentane, while both overpredicted for toluene and hexane. The models showed a mixture of this predictive behavior for dichloromethane and cyclohexane. It is thus difficult to state whether the evaporation rate calculated by these models is conservative or liberal. However, one can expect the computed evaportion rate by either model to be a reasonable approximation of the actual evaporation rate.

5.2 Validity of Raphael's Solar Insolation Relationship

During the course of the experiment, the solar insolation was recorded using a pyranometer located near the evaporation pan. These data were corrected for the reflectivity of the pool, based on the assumption that the reflective properties of the chemical is similar to that of water. This "corrected", or effective solar insolation was compared to the net solar insolation calculated from Raphael's relationship (Figure 2.2). Time averaged values of cloud cover and solar altitude were used to predict Raphael's net solar insolation under specific experimental time intervals.

It was found that Raphael's relationship slightly overpredicted the measured radiation in most cases by an average of 11%, which is excellent agreement, considering the simplicity of the prediction calculation. The actual differences between the measured and Raphael's values ranged from 0 to 31%. However, most of the "larger differences" occurred at relatively low solar altitudes or during periods of high fraction of cloud cover, when the solar insolation, and thus the absolute error, was small.

It is therefore suggested that Raphael's solar radiation curves can be used with confidence in predicting the solar insolation required for the two evaporation models, and for most environmental applications.

5.3 Mass Transfer Coefficients

The time averaged surface temperatures and the evaporation rates from the experiments were used to calculate the experimental mass transfer coefficients, using equation 1.1.

Table 5.2: Comparison of Mackay and Mastugu Mass Transfer Coefficient k(m), with Experimental k(ex)

Exp. No.	Chemical	10m Wind Speed km/h	k(m) m/h	k(ex) m/h	Dif %
1	Toluene	11.0	28.7	21.5	33
2	Toluene	14.0	33.1	34.0	3
3	Cyclohexane	6.2	17.2	23.1	26
4	Cyclohexane	7.7	20.5	23.5	13
5	Hexane	25.1	51.3	40.6	26
6	Dichloromethane	24.5	56.2	45.1	25
7	Dichloromethane	8.9	24.9	30.4	18
8	Pentane	10.0	24.5	37.5	35
9	Pentane	7.3	18.8	20.1	6
10	Pentane	8.0	20.2	17.2	17
11	Pentane	10.6	25.0	30.2	17

These values were compared with the Mackay and Mastugu correlation, which correlates the mass transfer coefficient as a function of the wind speed, length of the pool, and the chemical Schmidt number.

The calculated coefficients using this correlation were found to be lower than the experimental values by an average of 17% for two-thirds of the experiments and an average of 25% greater for the remaining experiments. This is not as accurate as desired, but the values were reasonable. Table 5.2 summarizes this comparison. There were no observable trends with respect to the chemical or the magnitude of the wind speed on the predictive behaviour of the correlation.

The mass transfer coefficient is one of the most important parameters and it is required with reasonable accuracy to successfully predict the behaviour of mass transport processes, such as evaporation. This can be seen in Table 5.3.

Table 5.3: Mass Transfer Coefficient and the Evaporation Rate

Data for Toluene: Experiment No. 2

		Predicted Evaporation Rate in kg/m2 h and Difference From Experimental Rate			
	k (m/h)	Direct Evap. Method		Surface Temp. Method	
k from correlation	28.7	4.70	(+39%)	4.39	(+30%)
k experimental	21.5	3.98	(+17%)	3.86	(+14%)

The evaporation rates were recalculated for experiment no. 2 by using the experimental mass transfer coefficient, keeping all other input parameters constant. It should be noted that in the surface temperature method, the heat transfer coefficient will be affected by this change in the mass transfer coefficient, as dictated by equation 3.2. It is clear from the comparison that a more accurate mass transfer coefficient will improve the prediction of the evaporation rate. Similar results can be obtained for other experiments, although the improvement is not as significant. Thus, further improvement in the model predictions is possible by formulating a more accurate mass transfer coefficient correlation.

However, the reason for not proceeding with this task is that the mass transfer coefficient may depend on solar insolation and other energy related terms, as well as the wind speed, the length and the Schmidt number. Inclusion of these additional parameters will be difficult to quantify and will

probably result in a more complicated relationship. It was decided, therefore, not to pursue a very accurate mass transfer coefficient and to continue to employ the existing correlation for the two evaporation models.

5.4 Validity and Discussion of the Use of Evaporation Models Under Spill Conditions

The evaporation models were developed using the assumption that the pool is at steady state and that the ground conduction effects are negligible. These assumptions, as well as the general applicability of the models in the actual spill situation are discussed in the following paragraphs.

The variation in the pool temperature following the spill can be described by identifying two distinct time periods. The initial period immediately following the spill can be viewed as an unsteady state period. Rapid changes in temperature take place in this period as the temperature of the chemical is brought from its initial or ambient temperature to the steady state temperature. This unsteady state behaviour teminates when the pool temperature remains relatively constant, and the time observed experimentally to arrive at this stage was approximately 15 minutes, as stated in Section 5.1. After this period, the pool can be viewed as being at steady state. There is no doubt that the pool temperature will continue to fluctuate during the steady state phase. However, any changes are relatively gradual and can be attributed to changes in atmospheric conditions, such as changes in the air temperature, solar insolation (for example, by a cloud passing in front of the sun), or the wind speed.

During the initial unsteady state period, the models will tend to underpredict the evaporation rate for volatile chemicals, since the steady state temperature (which the models are based) of the chemical pool will be lower than the ambient temperature. On the other hand, for non-volatile chemicals, the unsteady state period is not believed to be as significant. In the latter case, the models may be applied from the time immediately after the chemical is spilled.

In a real spill situation, the unsteady state period will probably have terminated before emergency crews arrive at the spill site. If one wishes to account for this effect, it is recommended that the initial temperature of the chemical, if known, or the air temperature be used to calculate the evaporation rate using equation 1.1. Steady state may be assumed 15 to 30 minutes after the spill, and either the direct evaporation or the surface temperature models should be applied. The evaporation rate should be re-evaluated periodically, using the up-to-date values for the air temperature, wind speed, and solar insolation.

It should also be noted that the effect of ground conduction, which was not taken into account in the two models, will diminish with time as the temperature difference between the pool and the ground diminishes. This effect is expected to be small after the initial unsteady state period described preivously, but experimental verification is required.

In the direct evaporation model, it was assumed that the net long-wave energy contribution is negligible. The results obtained from this model suggest that this assumption did not significantly affect the accuracy of the model when compared to the surface temperature model. This was also verified by the the calculated values of the difference between the long-wave radiation to and from the pool, which were relatively small in most experiments. One can also extend this result to the applicability of the two models to night-time spills. Despite the fact that there is no solar radiation at night, the net long-wave radiation energy is expected to be relatively similar in magnitude as during the day. Therefore, the two models could be used for both day and night-time spills. This may be particularly important to areas such as the Arctic, where the solar altitude is usually small.

Finally, it is believed that both the direct evaporation and the surface temperature models are applicable to non-volatile as well as volatile liquids. Experimental validation focused on volatile chemicals since these models include parameters which are important when dealing with volatile chemicals, such as solar insolation and evaporative cooling. These vairables are not as significant for non-volatile chemicals, but experimental verification of these two models with non-volatile chemicals should be undertaken.

5.5 Determining Which Model to Use

Since both the direct evaporation and surface temperature models were found to have similar accuracy and applicability, either model could be emloyed to predict the evaporation rate of chemical spills. The main advantage of both models is that the amount of input data required is small, and readily obtainable.

In terms of convenience, the direct evaporation method is the preferred model because it does not require a computer. It is thus useful for predicting the evaporation rate quickly. The surface temperature model, on the other hand, may prove to be valuable if a computer is available. More importantly, if the inclusion of the unsteady state ground conduction effects (and initial unsteady state effects) were to be implemented, the model best suited for this expansion would be the surface temperature model. Therefore, both models are useful, and the

model to use will likely depend on personal preference, convenience and application.

5.6 Exploratory Study of Evaporation From Snow

The snow-toluene "core" samples obtained from the snow evaporation experiment were divided into four equal layers, each representing a specific depth, from the first (top 1/4) to the last (bottom 1/4), as stated in Section 4.2. These samples were melted and analyzed for their toluene content. This enabled the determination of the toluene concentration at different snow depths.

The concentration profile of toluene with time at different depths is seen in Figure 5.2. In this figure, the concentration of toluene is represented by "percent to complete evaporation", which is the percent of the initial toluene evaporated at various sampling times. As expected, the top layer of snow resulted in the greatest toluene evaporation, while the smallest evaporation rate was observed in the bottom layer. The results indicate that a significant amount of toluene evaporated in the first 5 and 20 hours for the top and bottom layers, respectively. After this period, the amount evaporated was relatively insignificant. It was also found that almost all the toluene evaporated after the 48 hour period for the top 5 cm layer, but only 75% of the initial toluene evaporated in the same time period for the lowest layer. This difference is obviously due to the effect of added resistance to evaporation by increasing snow cover.

Similar trends in the toluene concentration were not obtained for the two intermediate depths. This was most likely due to poor sampling techniques, which resulted in compaction and thus, a certain degree of mixing of the different layers during collection of the snow samples. The collecting process was made more difficult by different degree of hardness of the snow-toluene mixture that was encountered at different sampling times. This variation in the hardness of the snow is attributed to slight melting and subsequent freezing of the snow during the 48 hour experimental period.

The overall percent of initial toluene which evaporated, averaged over the entire sample depth, was plotted against time in Figure 5.3. Also included in the figure is the evaporation rate of toluene from a pool of the same volume as the initial toluene content in the treated snow. This rate was predicted by using the direct evaporation model, using the 48 hour averaged values of the air temperature (-3 C), wind speed (23.6 km/h) and solar insolation (250 KJ/m2 h). The comparison of the overall depth-averaged evaporation rates from snow and from a pool is presented in Figure 5.4. This figure plots the ratio of the average evaporation rate from snow (cumulative) and the pool

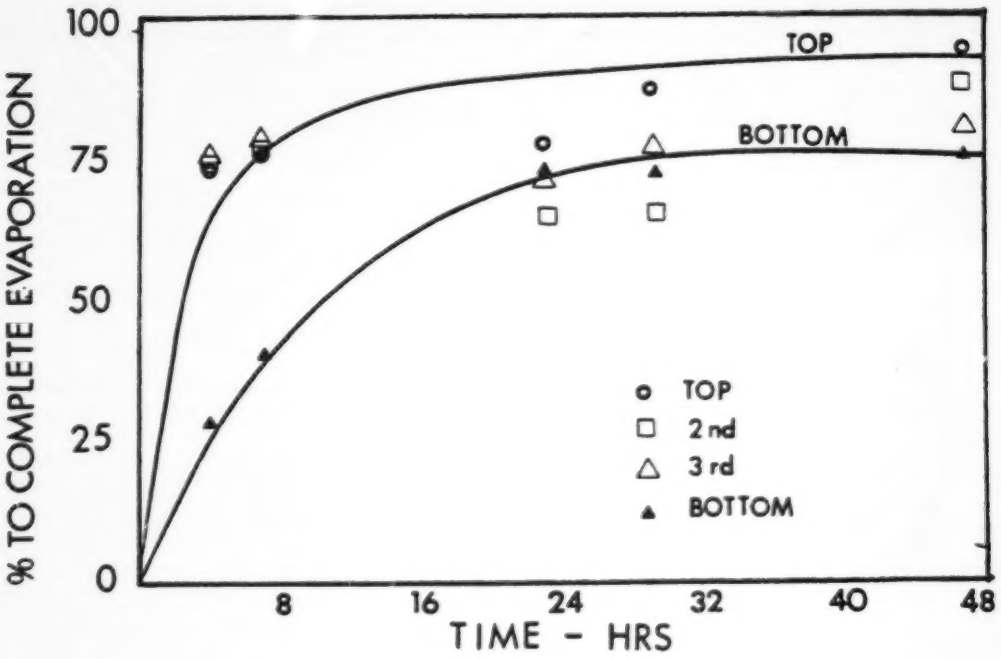

Figure 5.2: Evaporation of Toluene From Snow as a Function of Depth and Time

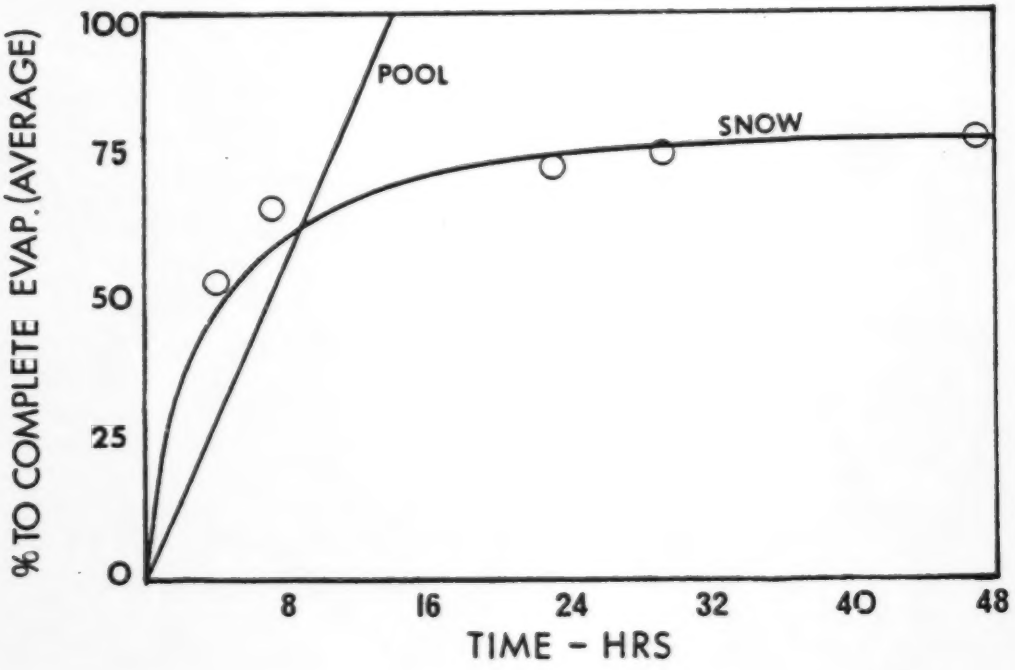

Figure 5.3: Depth-Averaged Evaporation of Toluene From Snow

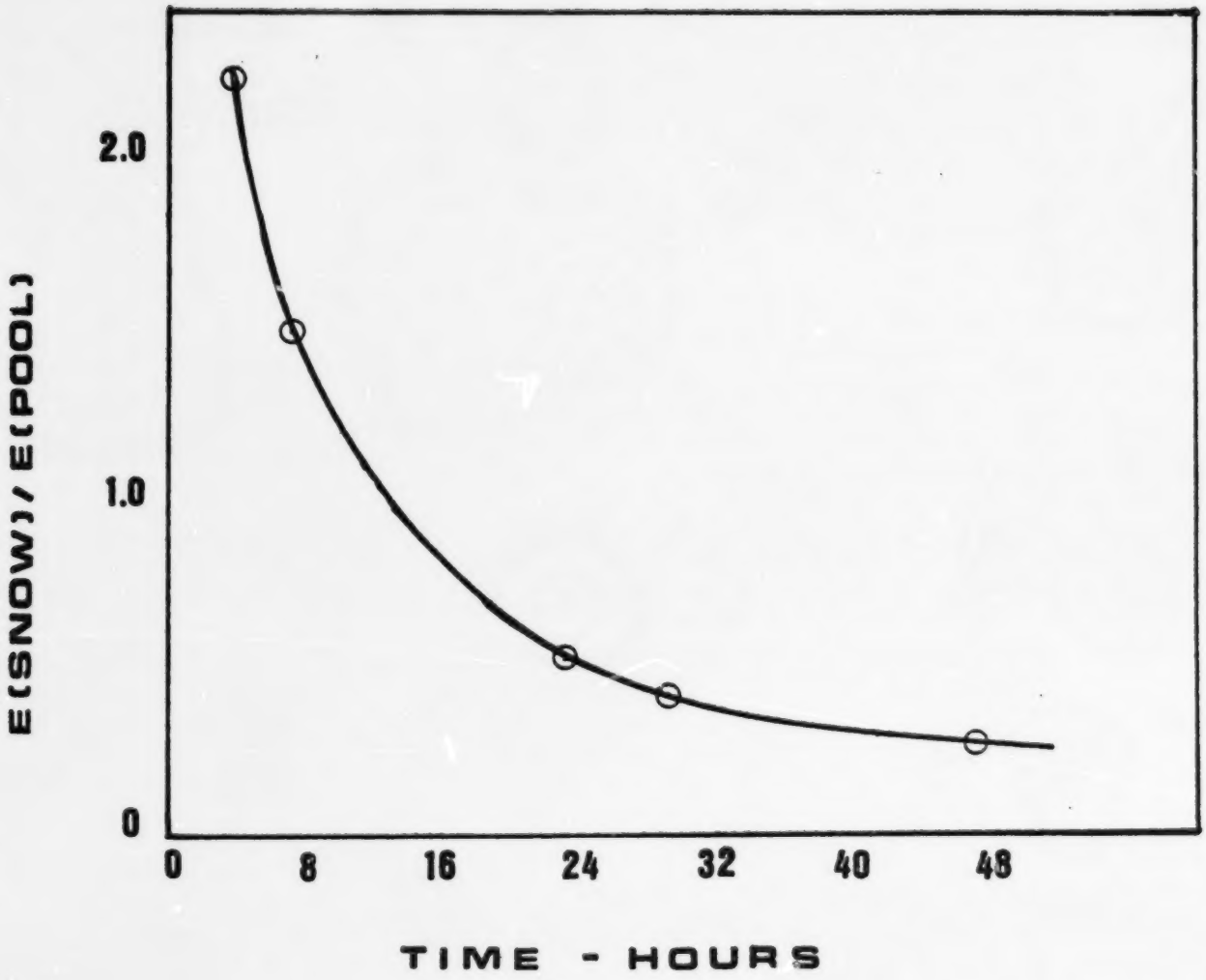

Figure 5.4: Comparison of the Overall Evaporation Rates From Snow (cumulative) and From a Pool

evaporation rate versus time.

The figures indicate that the average evaporation rate during the initial period was greater from snow than from a pool. There are two reasons to explain this unexpected result. First, the evaporation rate from a pool was calculated based on a 48 hour average wind speed of 23.6 km/h. If the actual initial wind speed of 35 km/h (averaged over the first 4 hrs of the experiment) was used, the predicted pool evaporation rate would be much greater, and will approach the magnitude of the initial evaportion rate from snow. Secondly, the very high rate of evaporation from snow, especially in the uppermost snow layer, is believed to be from the effect of increased surface area in which the air contacts the chemical. This effect is attributed to the non-uniform surface and to the porous properties of the snow. The greater evaporation rate from snow can thus be accounted for by the combination of these two effects.

After this initial period, the evaporation rate from snow becomes smaller than from a pool. This is because most of the chemical in the top layer has already evaporated, and most of the remaining chemical must now diffuse through the snow matrix in order to evaporate. The time at which the snow and pool rates are equal was found to be 13 hours after the spill.

It should be noted that all results presented in this section is based only on a single experiment, and more experiments are required before any generalizations can be made. Further research should address the effects of spills of different chemicals, involving different types and depths of snow. The sampling procedure should also be improved. It is hoped that this exploratory study will help in the design of a more thorough experimental study of this topic.

NOMENCLATURE

a	constant for vapour pressure equation	
b	constant for vapour pressure equation (b<0)	
B	atmospheric radiation factor	
Bo	Bowen's ratio	
c	constant for vapour pressure equation	
C	cloud cover factor	
Cpa	heat capacity of air	kJ/mol K
e	emissivity of the chemical	
D	declination	deg
E	evaporation rate per unit area	g/m2 h
EQ	equation of time	min
F	constant in surface temperature model	kJ/m2 h
h	hour angle of the sun	deg
Hvap	heat of vaporization	kJ/mol
k	mass transfer coefficient	m/h
L	longitude of the site	deg
LA	latitude of the site	deg
N	day number of the year	
P(t)	vapour pressure at temperature t	Pa
Patm	atmospheric pressure	Pa
Pa	partial pressure in air	Pa
Ps	partial pressure at the surface	Pa
Pr	Prandtl number	
Qatm	long-wave radiation from the atmosphere	kJ/m2 h
Qev	evaporation energy	kJ/m2 h
Qext	external heat source	kJ/m2 h
Qsen	sensible heat between pool and air	kJ/m2 h
Qsol	net solar radiation	kJ/m2 h
Qt	increase in energy stored in the pool	kJ/m2 h
r	reflectivity of long-wave radiation	
S	slope of vapour pressure curve at Ta	Pa/K
SA	solar altitude	deg
Sc	chemical Schmidt number	
t	temperature	C
T	absolute temperature	K
u	10 m wind speed	m/h
u*	friction velocity	m/h
U	heat transfer coefficient	kJ/m2 h C
X	pool diameter or length	m
y	height	m
yo	roughness length	m
Y	pressure conversion factor	
Z	constant in Bowen's ratio	Pa/K
ρa	density of air	mol/m3
σ	Stefan Boltzmann constant	kJ/m2 K4 h

REFERENCES

Air Weather Service. "Calculation of Toxic Corridors" AWS Pamphlet 105-57 (1978).

Anderson E.R. "Energy-Budget Studies, Water-Loss Investigations: Lake Hefner Studies" Professional Paper 269, Geol. Survey, US Dept of Interior, Washington, D.C. (1954).

Brutsaert W.H. "Evaporation into the Atmosphere" D. Reidel Publishing Co. Dordrecht, Holland, 1982.

Clewell H.J. "A Simple Formula for Estimating Source Strengths From Spills of Toxic Liquids" ESL-TR-83-03 (1983).

Fleischer M.T. "SPILLS-An Evaporation/Air Dispersion Model for Chemical Spills on Land", Shell Development Co. PB 83109470 (1980).

Gallant R.W. "Physical Properties of Hydrocarbons", Vol. 1, 2. Gulf Publishing Co. 1968.

Hooper F.C. Personal Discussion. Mechanical Engineering Dept. University of Toronto, 1984.

Ille G. and Springer C. "The Evaporation and Dispersion of Hydrazine Propellants from Ground Spills" CEEDO-TR-78-30 AD-A059407 (1978).

Kawamura P. and Mackay D. "The Evaporation of Volatile Liquids" Proceedings of the Technical Seminar on Chemical Spills, Tech. Services Branch, EPS. Toronto. (1985).

Kreith F., Kreider J.F. "Principles of Solar Engineering" Hemisphere Publishing Corp. Mc Graw Hill Co., 1978.

Kunkel B.A. "A Comparison of Evaporative Source Strength Models for Toxic Chemical Spills" Air Force Geophysics Lab.-TR-83-0307 (1983).

Lunde P.J. "Solar Thermal Engineering" John Wiley and Sons New York, 1980.

Mackay D. and Matsugu R.S. "Evaporation Rates of Liquid Hydrocarbon Spills On Land and Water" Can. J. Chem. Eng. 5 434, (1973).

Penman H.L. "Natural Evaporation from Open Water, Bare Soils and Grass" Proc. Roy. Soc. London A193, 120-146 (1948).

Phyper J.D. and Mackay D. "A Simple Micro-Computer Model of Short and Long Term Chemical Spill Behaviour on Land" Proceedings of the Technical Seminar on Chemical Spills, Tech. Services Branch, EPS. Toronto. (1985).

Raphael J.M. "Prediction of Temperature in Rivers and Reservoirs" Journal of the Power Division, Proc. of the American Society of Civil Engineers, 88 PO 2, (1962).

Stiver W., Mackay D. "Evaporation Rates of Spills of Hydrocarbons and Petroleum Mixtures" Environ. Sci. Technol. 18 834 (1984).

Whitacre C.G., Myirski M.M. "Computer Program for Chemical Hazard Protection" ARCSL-TR-822014 (1982).

Yaws C.L. "Physical Properties" McGraw Hill, New York. 1977.

ACKNOWLEDGEMENTS

The authors are grateful to Environment Canada, Transport Canada, and Natural Sciences and Engineering Research Council for financial support, and to the Atmospheric Environment Services branch in Downsview, Ontario for allowing us to conduct experiments at the AES site in Woodbrige, Ontario.

APPENDIX A TIME ZONE FACTORS

The time zone factor, tz, is required in equation 2.4, and is listed for some North American time zones.

Time Zone	Factor tz
EDT	+4
EST	+5
CST,MDT	+6
MST,PDT	+7
PST	+8

(Lunde, 1980)

APPENDIX B WIND VELOCITY CALCULATION

The first four experiments (experiment no. 1-4) were performed on the roof of the Chemical Engineering building in downtown Toronto. For these experiments, the hourly 10 m wind speed data obtained from the Toronto Island weather office were used as the wind speed for the models. The anemometer readings from the roof was not used because of the great turbulence created by the irregular roof surface, and nearby tall buildings made it difficult to calculate the "effective 10 m wind speed".

For experiments at the Atmospheric Environment Services site in Woodbridge, Ontario, the wind velocity obtained from the anemometer, located 0.35 m from the ground, was used. This velocity was converted to a 10 m wind speed by the following formula, which applies best for wind velocities near the earth's surface:

$$u = 2.5\, u^* \ln (y/yo)$$

where u is the wind speed, m/h
u* is the friction velocity, m/h
y is the height, m
yo is the roughness length, m.

Brutsaert (1982) lists values of yo as a function of various surfaces. For the AES site, the following values for yo were used:

i.	grass cover, no snow	yo = 2 cm
ii.	light snow cover	yo = 0.1 cm
iii.	heavy snow cover	yo = 0.01 cm

The anemometer readings, u, at a height of y = 0.35 m were used to calculate the friction velocity, u*, at a specified yo, using the above equation. Then the 10 m wind speed was calculated using the calculated value of u* (with the same yo). This calculated 10 m wind speed was used in the models.

APPENDIX C: EXPERIMENTAL DATA

Chemical	Toluene
Experiment No.	1
Date Performed	Sept 17 1984
Time of Experiment	13:00 - 14:00 EST
Data Averaged Over Period	1.0 hr
Pool Area (m)	0.657
Pool Depth (cm)	2.3
General Weather Description:	Sunny and Clear
Average Air Temp (C)	21.3
Average Pool Temp (C)	30.3
Average Surface Temp (C)	23.7
Calculated 10 m Wind Speed (m/h)	14000
Cloud Cover (%)	0
Average Solar Altitude (deg)	45
Vapour Pressure of Water (mbars) (from Relative Humidity)	26
Heat of Vaporization at Air Temp (kJ/mol)	38.1
Schmidt Number at Air Temp	1.86
Experimental Solar Insolation (kJ/m2 h)	2361
Predicted Solar Insolation (kJ/m2 h)	2385
Qback, Calculated (kJ/m2 h)	256
Qext, Calculated (kJ/m2 h)	12.6

APPENDIX C: EXPERIMENTAL DATA

Chemical	Toluene
Experiment No.	2
Date Performed	Aug 13 1984
Time of Experiment	15:10 - 16:10 EST
Data Averaged Over Period	1 hr
Pool Area (m)	0.292
Pool Depth (cm)	2.3
General Weather Description:	Sunny, with light thin cloud cover
Average Air Temp (C)	29.0
Average Pool Temp (C)	32.3
Average Surface Temp (C)	27.3
Calculated 10 m Wind Speed (m/h)	11000
Cloud Cover (%)	40
Average Solar Altitude (deg)	39.2
Vapour Pressure of Water (mbars) (from Relative Humidity)	26
Heat of Vaporization at Air Temp (kJ/mol)	37.9
Schmidt Number at Air Temp	1.86
Experimental Solar Insolation (kJ/m2 h)	1584
Predicted Solar Insolation (kJ/m2 h)	1820
Qback, Calculated (kJ/m2 h)	148
Qext, Calculated (kJ/m2 h)	3.8

APPENDIX C: EXPERIMENTAL DATA

Chemical	Cyclohexane
Experiment No.	3
Date Performed	Sept 19 1984
Time of Experiment	13:10 - 14:10 EST
Data Averaged Over Period	1.0 hr
Pool Area (m)	0.292
Pool Depth (cm)	2.2
General Weather Description:	Sunny and Clear
Average Air Temp (C)	24.0
Average Pool Temp (C)	17.1
Average Surface Temp (C)	12.5
Calculated 10 m Wind Speed (m/h)	6200
Cloud Cover (%)	10
Average Solar Altitude (deg)	43.3
Vapour Pressure of Water (mbars) (from Relative Humidity)	25
Heat of Vaporization at Air Temp (kJ/mol)	33.7
Schmidt Number at Air Temp	2.04
Experimental Solar Insolation (kJ/m2 h)	1930
Predicted Solar Insolation (kJ/m2 h)	1930
Qback, Calculated (kJ/m2 h)	7.2
Qext, Calculated (kJ/m2 h)	117

APPENDIX C: EXPERIMENTAL DATA

Chemical	Cyclohexane
Experiment No.	4
Date Performed	Sept 19 1984
Time of Experiment	14:10 - 15:10 EST
Data Averaged Over Period	1.0 hr
Pool Area (m)	0.292
Pool Depth (cm)	2.2
General Weather Description:	Sunny and Clear
Average Air Temp (C)	25.3
Average Pool Temp (C)	16.6
Average Surface Temp (C)	12.1
Calculated 10 m Wind Speed (m/h)	7700
Cloud Cover (%)	0
Average Solar Altitude (deg)	36.4
Vapour Pressure of Water (mbars) (from Relative Humidity)	25
Heat of Vaporization at Air Temp (kJ/mol)	33.7
Schmidt Number at Air Temp	2.03
Experimental Solar Insolation (kJ/m2 h)	1786
Predicted Solar Insolation (kJ/m2 h)	1820
Qback, Calculated (kJ/m2 h)	-22
Qext, Calculated (kJ/m2 h)	149

APPENDIX C: EXPERIMENTAL DATA

Chemical	Hexane
Experiment No.	5
Date Performed	Feb 27 1985
Time of Experiment	14:20 - 15:10 EST
Data Averaged Over Period	0.83 hr
Pool Area (m)	0.657
Pool Depth (cm)	2.4
General Weather Description:	Mainly Sunny, Windy Light Snow Cover
Average Air Temp (C)	-5.0
Average Pool Temp (C)	-8.1
Average Surface Temp (C)	-9.9
Calculated 10 m Wind Speed (m/h)	25100
Cloud Cover (%)	20
Average Solar Altitude (deg)	29.8
Vapour Pressure of Water (mbars) (from Relative Humidity)	4
Heat of Vaporization at Air Temp (kJ/mol)	33.3
Schmidt Number at Air Temp	1.91
Experimental Solar Insolation (kJ/m2 h)	1122
Predicted Solar Insolation (kJ/m2 h)	1400
Qback, Calculated (kJ/m2 h)	165
Qext, Calculated (kJ/m2 h)	81

APPENDIX C: EXPERIMENTAL DATA

Chemical	Dichloromethane
Experiment No.	6
Date Performed	Feb 27 1985
Time of Experiment	15:40 - 16:40 EST
Data Averaged Over Period	1.0 hr
Pool Area (m)	0.292
Pool Depth (cm)	2.3
General Weather Description:	Sunny with Cloudy Periods Windy, Light Snow Cover
Average Air Temp (C)	-6.3
Average Pool Temp (C)	-19.0
Average Surface Temp (C)	-25.0
Calculated 10 m Wind Speed (m/h)	24500
Cloud Cover (%)	40
Average Solar Altitude (deg)	18
Vapour Pressure of Water (mbars) (from Relative Humidity)	4
Heat of Vaporization at Air Temp (kJ/mol)	30.9
Schmidt Number at Air Temp	1.73
Experimental Solar Insolation (kJ/m2 h)	704
Predicted Solar Insolation (kJ/m2 h)	700
Qback, Calculated (kJ/m2 h)	-53
Qext, Calculated (kJ/m2 h)	200

APPENDIX C: EXPERIMENTAL DATA

Chemical	Dichloromethane
Experiment No.	7
Date Performed	Feb 25 1985
Time of Experiment	14:55 - 15:40 EST
Data Averaged Over Period	0.75 hr
Pool Area (m)	0.292
Pool Depth (cm)	2.2
General Weather Description:	Cloudy, Calm Light Snow Cover
Average Air Temp (C)	1.2
Average Pool Temp (C)	-14.4
Average Surface Temp (C)	-22.0
Calculated 10 m Wind Speed (m/h)	8900
Cloud Cover (%)	100
Average Solar Altitude (deg)	25
Vapour Pressure of Water (mbars) (from Relative Humidity)	4
Heat of Vaporization at Air Temp (kJ/mol)	30.2
Schmidt Number at Air Temp	1.80
Experimental Solar Insolation (kJ/m2 h)	230
Predicted Solar Insolation (kJ/m2 h)	300
Qback, Calculated (kJ/m2 h)	-185
Qext, Calculated (kJ/m2 h)	240

APPENDIX C: EXPERIMENTAL DATA

Chemical	Pentane
Experiment No.	8
Date Performed	Feb 20 1985
Time of Experiment	13:45 - 14:45 EST
Data Averaged Over Period	1.0 hr
Pool Area (m)	0.292
Pool Depth (cm)	2.4
General Weather Description:	Sunny with Cloudy Periods Heavy Snow Cover
Average Air Temp (C)	1.0
Average Pool Temp (C)	-19.2
Average Surface Temp (C)	-23.0
Calculated 10 m Wind Speed (m/h)	10020
Cloud Cover (%)	50
Average Solar Altitude (deg)	31
Vapour Pressure of Water (mbars) (from Relative Humidity)	5
Heat of Vaporization at Air Temp (kJ/mol)	27.8
Schmidt Number at Air Temp	2.11
Experimental Solar Insolation (kJ/m2 h)	953
Predicted Solar Insolation (kJ/m2 h)	1250
Qback, Calculated (kJ/m2 h)	-119
Qext, Calculated (kJ/m2 h)	527

APPENDIX C: EXPERIMENTAL DATA

Chemical	Pentane
Experiment No.	9
Date Performed	Nov 26 1984
Time of Experiment	15:30 - 16:00 EST
Data Averaged Over Period	0.5 hr
Pool Area (m)	0.292
Pool Depth (cm)	2.3
General Weather Description:	Light Cloud Cover (No Snow on Ground)
Average Air Temp (C)	5.0
Average Pool Temp (C)	-16.5
Average Surface Temp (C)	-19.2
Calculated 10 m Wind Speed (m/h)	7340
Cloud Cover (%)	20
Average Solar Altitude (deg)	8.0
Vapour Pressure of Water (mbars) (from Relative Humidity)	9
Heat of Vaporization at Air Temp (kJ/mol)	27.4
Schmidt Number at Air Temp	2.18
Experimental Solar Insolation (kJ/m2 h)	247
Predicted Solar Insolation (kJ/m2 h)	250
Qback, Calculated (kJ/m2 h)	125
Qext, Calculated (kJ/m2 h)	415

APPENDIX C: EXPERIMENTAL DATA

Chemical	Pentane
Experiment No.	10
Date Performed	Nov 26 1984
Time of Experiment	15:00 - 15:30 EST
Data Averaged Over Period	0.5 hr
Pool Area (m)	0.292
Pool Depth (cm)	2.3
General Weather Description:	Light Cloud Cover (No Snow on Ground)
Average Air Temp (C)	7.3
Average Pool Temp (C)	-8.6
Average Surface Temp (C)	-12.4
Calculated 10 m Wind Speed (m/h)	7970
Cloud Cover (%)	20
Average Solar Altitude (deg)	12
Vapour Pressure of Water (mbars) (from Relative Humidity)	9
Heat of Vaporization at Air Temp (kJ/mol)	27.4
Schmidt Number at Air Temp	2.15
Experimental Solar Insolation (kJ/m2 h)	386
Predicted Solar Insolation (kJ/m2 h)	350
Qback, Calculated (kJ/m2 h)	76
Qext, Calculated (kJ/m2 h)	390

APPENDIX C: EXPERIMENTAL DATA

Chemical	Pentane
Experiment No.	11
Date Performed	Nov 7 1984
Time of Experiment	15:45 - 16:15 EST
Data Averaged Over Period	0.5 hr
Pool Area (m)	0.292
Pool Depth (cm)	2.1
General Weather Description:	Very Light Cloud Cover, Hazy (No Snow Cover)
Average Air Temp (C)	9.0
Average Pool Temp (C)	-16.9
Average Surface Temp (C)	-18.9
Calculated 10 m Wind Speed (m/h)	10600
Cloud Cover (%)	20
Average Solar Altitude (deg)	9.1
Vapour Pressure of Water (mbars) (from Relative Humidity)	5
Heat of Vaporization at Air Temp (kJ/mol)	27.4
Schmidt Number at Air Temp	2.18
Experimental Solar Insolation (kJ/m2 h)	293
Predicted Solar Insolation (kJ/m2 h)	300
Qback, Calculated (kJ/m2 h)	-151
Qext, Calculated (kJ/m2 h)	740

APPENDIX D

COMPUTER PROGRAM - DIRECT EVAPORATION MODEL

```
10 PRINT "CHEMICAL IS"
20 INPUT CHEM$
30 PRINT "MOLECULAR WEIGHT IS"
40 INPUT M
50 PRINT "AIR TEMP IS IN C"
60 INPUT TA
70 PRINT "EXTERNAL HEAT SOURCE IS (KJ/M2 H)"
80 INPUT QEXT
90 PRINT "PRESSURE CONVERSION FACTOR TO Pa IS"
100 INPUT Y
110 PRINT "HEAT OF VAPORIZATION IS (KJ/MOL)"
120 INPUT HVAP
130 PRINT "CONSTANT  FOR VAPOUR PRESS EQUATIONS...A "
140 INPUT A
142 PRINT "CONSTANT B FOR VAP PRES EQTN: ENTER B AS NEGATIVE"
145 INPUT B
150 PRINT "CONSTANT C IN VAPOUR PRESS EQUATION IS"
160 INPUT C
170 PRINT "EVAPORATION AREA IS (M2)"
180 INPUT AREA
190 PRINT "AVERAGE SOLAR ALTITUDE IS (DEGREES)"
200 INPUT ALPHA
210 PRINT "AVERAGE CLOUD COVER IS (0 FOR NO CLOUD; 10 FOR COMPLETE CLOUD)"
220 INPUT CLOUD
230 LET ALPHAR=ALPHA*3.14/180
240 LET QSS=(1-(.0071*(CLOUD)^2))
250 LET QSOL=4000*QSS*(SIN(ALPHAR)-.1)
260 PRINT "MASS TRANSFER COEFFICIENT IS (M/H)"
270 INPUT K
280 PRINT "THE SCHMIDT NO IS"
290 INPUT SC
300 LET Z=3650*(SC)^.67/HVAP
310 LET PRE=EXP(2.3*(A+(B/(TA+C))))
320 LET S=Y*PRE*(-B/(TA+C)^2)
330 LET Q=(QSOL+QEXT)*M/HVAP
340 LET DEN=Z+S
345 LET ETA=PRE*Y*M*K/(8.314*(TA+273))
350 LET E=(S*Q/DEN) + (Z*ETA/DEN)
360 PRINT CHEM$
370 PRINT "THE PREDICTED EVAP RATE IS, IN G/M2 H ", E
380 PRINT "THE PREDICTED EVAP RATE IS, IN G/H", E*AREA
430 END
```

APPENDIX E

COMPUTER PROGRAM - SURFACE TEMPERATURE MODEL

```
10 PRINT "CHEMICAL IS"
20 INPUT CHEM$
30 PRINT "MOLECULAR WEIGHT IS"
40 INPUT M
50 PRINT "AIR TEMPERATURE IS (C)"
60 INPUT TA
70 LET TA=TA+273
80 PRINT "EXTERNAL HEAT SOURCE IS (KJ/M2 H)"
90 INPUT QEXT
100 PRINT "PRESSURE CONVERSION FACTOR TO Pa IS"
110 INPUT Y
120 PRINT "HEAT OF VAPORIZATION IS (KJ/MOL)"
130 INPUT HVAP
140 PRINT "CONSTANT A FOR VAPOUR PRESS EQTN IS "
150 INPUT A
152 PRINT "ENTER CONSTANT B (AS NEGATIVE) FOR VAP PRES EQTN"
155 INPUT B
160 PRINT "CONSTANT C IN VAPOUR PRESS EQUATION IS"
170 INPUT C
180 PRINT "EVAPORATION AREA IS (M2)"
190 INPUT AREA
200 PRINT "AVERAGE SOLAR ALTITUDE IS"
210 INPUT ALPHA
220 PRINT "AVERAGE CLOUD COVER IS (0 FOR NO CLOUD,; 10 FOR COMPLETE CLOUD)"
230 INPUT CLOUD
235 LET ALPHAR=ALPHA*3.14/180
240 LET QSS =(1-(.0071*(CLOUD)^2))
242 LET QSOL=4000*QSS*(SIN(ALPHAR)-.1)
250 PRINT "ATMOSPHERIC RADIATION FACTOR IS"
260 INPUT BETA
270 PRINT "MASS TRANSFER COEFFICIENT IS (M/H)"
280 INPUT K
290 PRINT "HEAT TRANSFER COEFFICIENT IS (KJ/M2 H K)"
300 INPUT U
310 LET QATM=BETA*1.98E-07*TA^4
320 LET QSEN = U*TA
330 LET F=QSOL+QATM+QEXT
340 PRINT "INPUT INITIAL GUESS OF TS IN C (USUALLY AIR TEMP)"
350 INPUT TS
360 LET TS=TS+273
370 LET N=0
380 LET DT=1.1
390 IF ABS(DT)<=.5 OR N>24 THEN 540
400 LET QSUR=1.98E-07*TS^4
410 LET QSENS=U*TS
420 LET PRES=EXP(2.3*(A+(B/(TS-273+C))))
430 LET QEV=Y*K*HVAP*PRES/(8.314*TS)
440 LET INB=F-QEV-QSUR+QSEN-QSENS
450 LET DQSUR=7.92E-07*TS^3
460 LET DQSENS=U
470 LET DQEV=Y*K*HVAP*(PRES*(1/TS)*((-1/TS)-(B/(TS-273+C)^2)))/8.314
480 LET SUM=ABS(DQSUR)+DQSENS+ABS(DQEV)
490 LET DT=INB/SUM
500 LET TSOLD=TS
510 LET N=N+1
520 LET TS=TSOLD +DT
530 GOTO 390
540 PRINT CHEM$
550 PRINT "THE PREDICTED SURFACE TEMP IS";TS-273
560 PRINT "THE NO OF ITERATIONS ";N
570 PRINT
580 PRINT "THE PREDICTED EVAP RATE IS, IN G/H";QEV*M*AREA/HVAP
590 PRINT "THE PREDICTED EVAP RATE IS, IN G/M2 H";QEV*M/HVAP
600 END
```